



COMBINED EFFECTS OF INFILL WALLS AND STEEL BRACINGS IN SEISMIC RESPONSE OF RC BUILDINGS

Anastasios ANDREADAKIS¹ and Yiannis TSOMPANAKIS²

ABSTRACT

The present study is focused on seismic vulnerability assessment and retrofitting of typical reinforced concrete (RC) buildings that were designed and constructed according to the common practice and simplistic provisions in 60's and 70's in Greece as well as in other seismic prone European countries. For this purpose, the characteristic SPEAR building was chosen that has been extensively examined experimentally and numerically. The examined modes of this structure include infill panels and additional steel bracings in selected bays of the frame, thus, several modelling scenarios were considered consisting of variant arrangements of infill panels and brace members. Response parameters are analysed (mainly concerning the global behaviour of the structure) to investigate the sensitivity of the results when adopting various values of the mechanical parameters of infill walls which have many inherent uncertainties, hence, creating difficulties in obtaining realistic results. The impact of the combined action of infill walls and steel bracings is thoroughly investigated through non-linear static (pushover) analyses.

1. INTRODUCTION

The majority of reinforced concrete (RC) buildings in seismic prone regions has been designed and constructed before modern seismic norms were introduced, i.e., fulfilling much lower capacity and seismic demand requirements. As a consequence, efficient retrofitting strategies have to be implemented in order to achieve the desired performance levels following the principles of contemporary performance-based design (PBD). An efficient method of upgrading the bearing structure and increasing its overall capacity against seismic loading conditions is the use of steel bracings in selected bays of the RC frame. Guidelines for the implementation of this strengthening technique are provided in the recently introduced Greek retrofitting norm (KAN.EPE 2013) in combination with Eurocode 8 – Part 3 (EN1998-1-3 2005).

Infill walls usually play a more crucial role in existing (as they were designed with past norms, they are in general more flexible as they do not have stiff RC walls, their columns may have local problems from increased shear forces due to infills, etc) than in new RC structures (where issues related to infills' potential adverse effects should taken into account during the design (Eurocode 8 – Part 1 (EN1998-1-1 2004)), should be included in the computational simulations in a suitable manner. Consequently, over the last decades significant research effort has been focused on the impact of infill walls in RC frames in order to assess current structural condition. Especially for buildings with a

¹ PhD Student, School of Environmental Engineering, Technical University of Crete, Chania, Greece
aandreadakis@isc.tuc.gr.

² Associate Professor, School of Environmental Engineering, Technical University of Crete, Chania, Greece, jt@science.tuc.gr.

pilotis-type ground floor (i.e., without infills) and infills in the upper storeys, which are in general more susceptible to the development of soft story mechanism due to stiffness irregularity (Mondal and Tesfamarian 2014). There are also several studies that have been focused on the use of steel bracings for retrofitting of existing RC frames only in the ground floor (e.g., Antonopoulos and Anagnostopoulos 2013), or along the height of the building.

In the present work, the combined effects of these two important issues are studied in order to investigate the sensitivity in modelling both types of element (infill walls and steel braces) that have a different behaviour during seismic loading, while they have to act in an integrated manner. For this purpose, a parametric study has been performed utilizing a prototype RC structure (SPEAR building) shown in Fig. 1 that has been well studied by various researchers (SPEAR 2005; Dolsec and Fajfar 2005; Fragiadakis et al. 2009). The results obtained via advanced numerical simulations utilizing OpenSees (McKenna et al. 2000) are compared and the differences of each examined case are highlighted. The modelling parameters used in experimental tests of the original SPEAR building were modified and fitted to the purposes of this study.

In particular, several different modelling scenarios have been developed that include masonry infill walls and steel braces in selected locations within certain bays of the RC frame in which some of the mechanical parameters of the infill walls are modified in each analysis in order to compare the results. The examined cases are in brief as follows:

- i) “Fully infilled” structure: Infill walls placed at all the stories at all the bays of the frame.
- ii) “Open ground floor”: Infill walls were modelled in the upper two stories.
- iii) “Scenario br1”: No infill walls at the ground floor and steel braces in two selected bays of both directions at the ground floor, namely the bays of beams B1, B5 and B8, B12 (see Fig. 1) along both directions of the structure.
- iv) “Scenario br2”: No infill walls at the ground floor and steel braces placed at all the stories within two selected bays of both directions, i.e., bracings were placed at the same bays B1, B5 and B8, B12 but along the whole height of the building.

The perspective views of the four modelling scenarios that were described above are shown in Figs. 2 and 3.

Emphasis is given on the investigation of the sensitivity of the results due to the dispersion of the mechanical parameters of the infill walls. Hence, the modelling assumptions and the element types that are used in the RC frame model are kept constant during the analyses, while the parameters of the infill wall model are modified. Simulation and assessment were based on contemporary seismic design and retrofitting guidelines in Europe (EC8 - Part 1 2004 and EC8 - Part 3 2005) and, in particular, in Greece (KAN.EPE 2013). It is well-known that the mechanical characteristics of infill walls have a large scattering even in the same structure, because of not fulfilling any specific standards during the construction as well as due to the lack of proper standardization for the production of clay bricks that are mainly used for infills. As a consequence, the mechanical characteristics of infill walls have a high uncertainty level and it is very common that their values vary significantly all over the structure and maybe even in the same frame opening.

Modal and non-linear static analyses have been performed in order to assess the response of the structure with respect to the variations of the modeling parameters. The interpretation of the obtained results was focused mainly to illustrate their global impact on the structure according to performance-based design (PBD) viewpoints. The present investigation demonstrates the complexity and difficulties to predict a priori the efficiency of any strengthening intervention. The findings of the study highlight various crucial issues that affect the effectiveness of steel bracings retrofitting strategy in conjunction with the influence of the infills.

2. DESCRIPTION OF THE EXAMINED STRUCTURE

The examined structure (SPEAR building) is a three storey RC building designed according to the seismic design principles similar to those used in 60’s and 70’s in Greece (actually up to 1984 where the Greek seismic norm was reformed and adopted important principles related to ductility, etc) as well as in other European countries, therefore it is primarily designed to withstand gravity loads. The

main defects and deficiencies that characterize this type of structures are: poor detailing of the critical regions, inadequate transversal reinforcement, insufficient anchorage of the reinforcement bars, poor quality of materials (concrete and steel reinforcement), the absence of capacity design, etc.

The typical floor plan and the reinforcements of beams and columns are depicted in Fig. 1. All columns have rectangular cross-sections with dimensions (in cm) 25x25, except a rectangular one that has a cross-section of 25x75, while all beams have dimensions 20x50. For the steel braces a square hollow section 180x180x12 was used. Finally, the thickness of the infill walls is set equal to 20cm, while it was assumed that there are no openings at the walls.

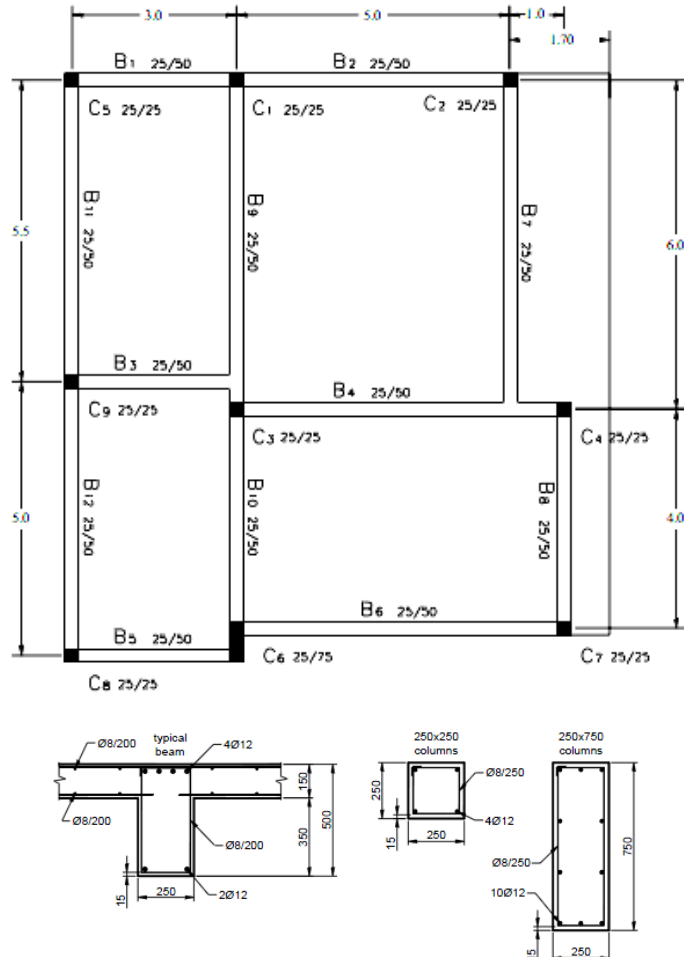


Figure 1. Typical floor plan and member's reinforcements (Dolsec and Fajfar 2005)

The longitudinal reinforcement of the ending regions and the effective width of the beams are shown in Table 1. As it can be observed from the data listed there, the reinforcement of beams that are located in the effective width of the beams contributes to bending behaviour and they have been taken into account in the calculations of the moment-curvature response diagram ($M-\phi$) of each beam.

The moment-curvature diagrams are calculated utilizing software RCCOLA.NET (Kappos and Panagopoulos 2009) that takes into account several parameters (i.e., failure criteria) in order to obtain the “equivalent” and monotonic bilinear curve. These parameters/criteria are: i) buckling of reinforcement bars under compression, ii) hoop fracture due to a strain arising from expansion of confined core, iii) drop of concrete stress to $0.85f_c$ along the descending branch of the $\sigma_s-\epsilon_c$ diagram, and iv) fracture of the longitudinal reinforcement in the tension zone due to exceeding the ultimate strain ϵ_{su} .

The building is regular in elevation, as it has equal floor dimensions in all stories and has a total height 8.75m (2.75m in 1st storey and 3.00m in each of the upper two stories). It can be assumed that is irregular in plan, to some extent, due to the distance between the center of mass and the center of

rigidity. Actually, this correlation between the two points is just one parameter that indicates the irregularity in plan of the building, yet it is not a unique sufficient condition. According to Eurocode 8 – Part 1 (EN1998-1-1 2004) there are two conditions that have to be fulfilled in order to characterize a building as regular in plan:

$$e_{ox(oy)} \leq 0.30 * r_{x(y)}, \quad r_{x(y)} \geq l_s \quad (\text{in both directions}) \quad (1)$$

where $e_{ox(oy)}$ is the static eccentricity (i.e., the distance between the center of mass and the center of rigidity), $r_{x(y)}$ is the “torsional radius” and l_s is the radius of gyration of the floor mass in plan.

It should be noted that in Eurocode 8 - Part 1 the suggested way that the two quantities of e_{ox} and r_x are calculated for multistory buildings is a crude approximation (as it is stated in section 4.2.3.2 of EC8 - Part 1) and a most proper way is being used in latest Greek seismic norm (EAK 2003), which employs the “fictitious elastic center” instead of the center of rigidity. This method is also adopted herein, to obtain an additional parameter for the qualitative assessment of the structure’s overall behavior. Additionally, in this manner the examined building model can be characterized according to the Greek norm based on its regularity in plan. Since the aforementioned two conditions are fulfilled (considering the frame without simulating the infill walls and steel braces), thus, the building is neither irregular in plan or “torsional sensitive” (note that in EC 8 - Part 1 the term “torsional flexible” is used instead). For this verification, a commercial technical software (RAF-TOL 2013) was used and the results of the calculations are shown in Table 2. In any case, the importance of the torsional effects on the overall behavior of the structure cannot be ignored (which, in general, they are more important for the bare structure).

Table 1. Longitudinal reinforcement of ending regions and effective width of beams (Dolsec and Fajfar 2005)

Beam (# i)	Effective width (cm)	bottom	Reinforcement top web	top slab	Beam (# j)	Effective width (cm)	bottom	Reinforcement top web	top slab
B1	75	2Φ12	2Φ12, 2Φ12	3Φ8	B1	75	2Φ12	2Φ12, 4Φ12	8Φ8
B2	125	2Φ12	2Φ12, 4Φ12	13Φ8	B2	125	2Φ12	2Φ12, 2Φ12	15Φ8
B3	150	2Φ12	2Φ12, 4Φ12	8Φ8	B3	150	2Φ12	2Φ12, 2Φ12	8Φ8
B4	175	3Φ20	2Φ12, 4Φ20	14Φ8	B4	175	5Φ20	2Φ12	3Φ8
B5	75	2Φ12	2Φ12, 2Φ12	3Φ8	B5	75	2Φ12	2Φ12, 2Φ12	3Φ8
B6	150	2Φ12	2Φ12, 2Φ12	11Φ8	B6	150	2Φ12	2Φ12, 2Φ12	11Φ8
B7	300	2Φ12	2Φ12, 3Φ20	25Φ8	B7	150	2Φ12	2Φ12, 3Φ20	7Φ8
B8	125	2Φ12	2Φ12, 2Φ12	6Φ8	B8	125	2Φ12	2Φ12, 2Φ12	6Φ8
B9	175	2Φ20	4Φ12, 1Φ20	13Φ8	B9	200	2Φ20	2Φ12, 2Φ20	9Φ8
B10	125	2Φ12	4Φ12	6Φ8	B10	125	2Φ12	4Φ12, 2Φ20	8Φ8
B11	137.5	2Φ12	2Φ12, 4Φ12	9Φ8	B11	75	2Φ12	2Φ12, 2Φ12	2Φ8
B12	75	2Φ12	2Φ12, 2Φ12	2Φ8	B12	125	2Φ12	2Φ12, 4Φ12	9Φ8
B13	175	3Φ20	2Φ12, 1Φ20	18Φ8	B13	112.5	3Φ20	2Φ12, 3Φ20	9Φ8
B14	175	2Φ12	4Φ12, 2Φ20	19Φ8	B14	175	2Φ12	4Φ12, 2Φ20	19Φ8

Table 2. Results for the classification of regularity in plan (bare structure)

Storey	e_{ox}	e_{oy}	r_x	r_y	l_s	$0.30 * r_x$	$0.30 * r_y$
1st	0.86	0.92	4.76	5.68	3.85	1.428	1.704
2nd	0.86	0.92	4.76	5.68	3.85	1.428	1.704
3rd	0.98	0.97	4.78	5.69	3.86	1.434	1.707

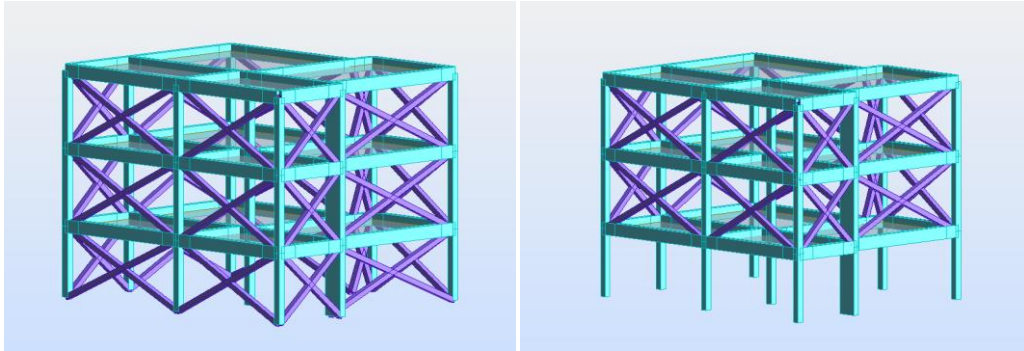


Figure 2. Perspective views of modeling scenarios “fully infilled” and “open ground floor” (infills shown with diagonal struts)

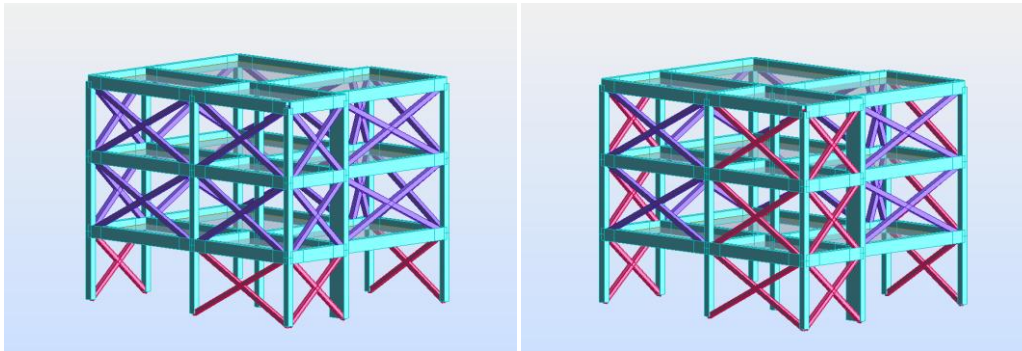


Figure 3. Perspective views of modeling scenarios br1 and br2 (steel braces in red, infills' struts in blue)

The self weight of the RC members and slabs was calculated considering a unit weight equal to 25.0kN/m^3 , while for masonry infill walls it was equal to 18.0kN/m^3 . Gravitational loading for the seismic load combinations assumed as $G+0.30*Q$, where G denotes the permanent load (self weight of RC members and slabs + 0.50kN/m^2 and also infill walls and braces) and Q is the live load set equal to 2.00kN/m^2 . The tributary gravitational loads were assigned to beams and assumed to be uniformly distributed along each beam's clear span. The mass of each floor was determined according to EC8 – Part 1 and corresponded to loads derived from the $G+0.30*Q$ combination. Translational masses and mass moment of inertia are concentrated and applied at the center of mass of each floor (in which the nodes of each floor are constrained).

3. NUMERICAL MODELLING DETAILS

The examined structure has been simulated adopting modelling options that are used in specialized earthquake engineering software, such as the popular OpenSees open-source platform that has been used in the present study. Although modelling parameters of certain structural elements (the ones used to simulate infill walls and steel braces) were intentionally not extremely sophisticated, since the aim was to reproduce the common practice of using -in a relatively simplistic manner due to various limitations- available computational tools.

The material properties used in the numerical models were derived from the post-test model of the SPEAR building (Dolsec and Fajfar 2005) in conjunction with some other data obtained from the half-scale experiment that took place on the shake table of TREES laboratory at EUROCENTER in Pavia, Italy (Fragiadakis et al. 2009). More specifically: i) for the strength of concrete f_{ck} the mean value was used for all RC members: $f_{ck}=25$ MPa, ii) the tensile strength of the reinforcing steel f_y is taken equal to 293 MPa to take into account, in an average manner, the simulation of slippage of reinforcement (by reducing the yield strength of longitudinal reinforcement that initially had a higher value). The modulus of elasticity of concrete was equal to $E_c=25$ GPa ($=2.0*f_c/\epsilon_{cu}$). The masonry of

the infill walls was assumed to have $f_m=2.20$ MPa vertical compressive strength, $f_h=1.80$ MPa horizontal compressive strength and $t_{cr}=0.20$ MPa (initial) shear strength, while the modulus of elasticity of the masonry was equal to $E_{inf}=1600$ MPa. The characteristic tensile strength of steel braces f_{sy} was equal to 235 MPa and the elasticity modulus E_s was equal to 210 GPa.

The finite element simulation of the non-linear response of both columns and beams in this study is based on the distributed plasticity approach, in which the development of plastic hinges is allowed in any location along the member (with respect to the defined integration points). For the beams the “displacement-based” element (DBE) formulation is used because of the discretization of members that has already taken place due to the differentiation of reinforcement arrangements at the ends and the middle region of the beams (see Table 1). Furthermore, uniaxial constitutive relationship of the sections is assigned at the integration points of each displacement-based element according to the M-φ diagrams that are previously defined (via RCCOLA.NET software). This simulation approach for beams, among others, allows considering each floor as a rigid diaphragm at its plane (which constitutes a very realistic assumption for the specific building). Note that the use of fiber elements for the simulation of beams in combination with the use of rigid diaphragm leads to the development of unrealistic and non-desirable axial forces, due to shifting of the neutral axis, and thus to unreliable moment capacity calculations.

On the other hand, the “force-based” element (FBE) is used for the columns, in which a single element per member is only needed to simulate its non-linear response (which is realistic due to the constant reinforcement arrangement along the columns). In general, this is a more accurate approach compared to the displacement-based elements. In addition, fiber sections are used for the definition of the force-based elements, which are superior for the simulation of the vertical members, as they take into account more effectively the P-M-M (i.e., axial force and biaxial moment) interaction at material level. This is very important due to the fact that the axial forces play a crucial role in member’s bending capacity, while this interaction is continuously updated at each step of the analysis.

The shear and torsional behavior of all members is assumed to be elastic (regarding torsion, a 50% reduction of stiffness was assumed). Furthermore, the P-Delta effects are taken into account through the definition of the co-rotational coordinate transformation in columns. Centerlines are used for the horizontal members, i.e., the beams are connected directly with the nodes of the columns without defining rigid offsets (except the beams that are connected with rectangular column C6, of dimensions 25x75, where rigid elements are used to account for the proper geometry arrangement of the connection area) to account for additional deformations not modeled directly (i.e., bar slippage and joint shear distortion).

The uniaxial constitutive relationships of each of the two materials (concrete and steel) that compose every section of the FBE of columns are shown in Fig. 4. More specifically, these are: a) the Kent-Scott-Park law for concrete fibers that allows for a quite accurate prediction of the demand for flexure dominated RC members (Fig. 4a), and b) a bilinear model with pure kinematic hardening for steel fibers (Fig. 4b).

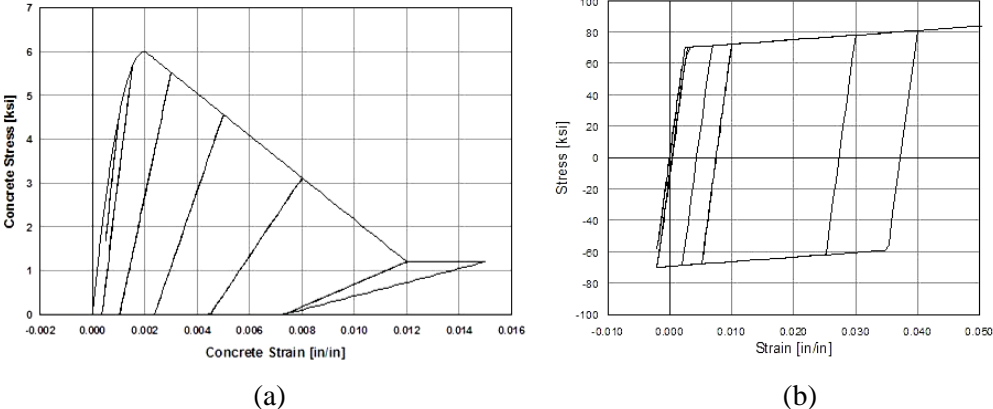


Figure 4. a) Typical stress-strain relation according to Kent-Scott-Park model adopted for concrete fibers; b) Bilinear model with pure kinematic hardening used for steel fibers

As it was previously mentioned, the masonry infill walls were simulated in a rather typical manner, by introducing two diagonal compressive-only struts (truss elements) as shown in Figs. 2 and 3, while the local effects on the surrounding RC frame were not taken into account. The non-linear force-displacement relationship of the struts follows the same rule as it was assumed for the material of the concrete fibers of columns, as it is considered a sufficient way to include most sources of material deterioration (Hashemi and Mosalam 2006). The response diagram adopted for infills is depicted in Fig. 5.

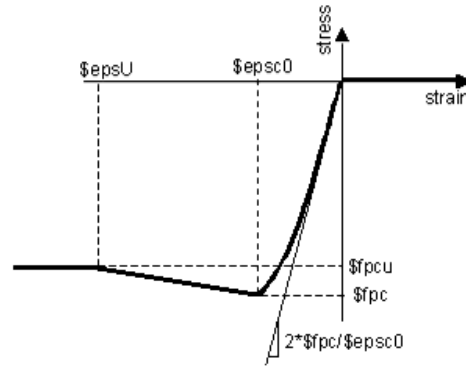


Figure 5. The Kent-Scott-Park model adopted for masonry infill walls

In this study, the formulation proposed by Zarnic and Gostic (1997) is adopted for the calculation of the maximum strength of the infill f_{pc} (in terms of force):

$$f_{pc} = 0.818 \cdot \frac{L_n \cdot t_w \cdot f_{tp} \cdot (1 + \sqrt{C_1^2 + 1})}{C_1}, \quad C_1 = 1,925 \cdot \frac{L_{net}}{H_{net}} \quad (2)$$

where L_{net} , H_{net} are the net dimensions of the infill, t_w is the wall thickness, f_{tp} is the cracking strength of the infill. The displacement at the maximum lateral force is estimated by (in terms of length):

$$e_{psc0} = \frac{\varepsilon_m \cdot \sqrt{L_{net}^2 + H_{net}^2}}{\cos \theta} \quad (3)$$

in which ε_m is the masonry compression strain (of the inclined strut) at the maximum compression stress and θ is the inclination of the diagonal. The initial stiffness α_{el} is taken as:

$$\alpha_{el} = 2 \cdot \left(\frac{f_{pc}}{e_{psc0}} \right) \quad (4)$$

Typically, the post yielding slope α_c can be assumed equal to 10% of α_{el} , while the stress at the ending point of the stress-strain diagram (i.e., the residual strength, e.g., Hashemi and Mosalam (2006)) is taken equal to 8% of f_{pc} .

The analytical investigation of the calculation of the mechanical parameters of infills is beyond the scope of this work, thus, many of the partial quantities that form the final values of f_{pc} and e_{psc0} are ignored (a thorough guidance about this matter is provided in Greek guidelines for structural upgrading interventions (KAN.EPE 2013)). The values for the basic parameters for the simulation of the struts that are modified during the analyses (for the four examined scenarios) are: i) ε_m takes values of 0.0010, 0.0012 and 0.0014, and ii) f_{tp} ($=t_{cr}$, assuming that shear failure is the predominant failure type) that takes values of 0.20, 0.24 and 0.28. This variation (20% increase of the value in each case) actually represents the scaling of the performance level that correlates the final adopted values of the mechanical parameters of infill walls with the displacements and the tolerable damage level of infills.

The simulation of the steel braces follows the provisions of the Greek norm for structural upgrading interventions (KAN.EPE 2013). The type of elements that are used for this purpose is truss elements with a trilinear constitutive law for the force-displacement relationship as it is shown in Fig. 6. The main quantities that define this model are: i) $F_y^{(+)}$ representing the yielding point of steel member under tension; ii) $F_y^{(-)}$ representing the resistance of steel member under compression (i.e., the buckling resistance); iii) $D_y^{(+)}$ and $D_u^{(+)}$ are the displacements that correspond to the yielding point under tension and to the ultimate value for member under tension, respectively; iv) $D_y^{(-)}$ and $D_u^{(-)}$ are the displacements that correspond to the buckling resistance and to the ultimate value for member under compression, respectively. The resistance that corresponds to the ending point (positive or negative) of the trilinear curve is equal to zero, thus, once displacement reaches the values of $D_y^{(-)}$ or $D_u^{(-)}$ then fracture of the member occurs (note that in OpenSees script this behavior is modeled through the MinMax material). The formulas that are used for the calculation of the above values (according to (KAN.EPE 2013)) are:

$$F_y^{(+)} = f_y * A / \gamma_M, \quad F_y^{(-)} = 0.20 * N_b / \gamma_M \quad (5)$$

$$D_y^{(+)} = L * F_y^{(+)} / (E * A), \quad D_y^{(-)} = L * N_b / (E * A), \quad D_u^{(+)} = 12 * D_y^{(+)}, \quad D_u^{(-)} = 10 * D_y^{(-)} \quad (6)$$

where N_b is the buckling resistance that is correlated with Euler's buckling load N_{cr} given in EC-3 (EN 1993-1-1 2005). The effective buckling length is taken as the half of the total length of the brace assuming that the two crossing braces are connected in the middle with a gusset plate.

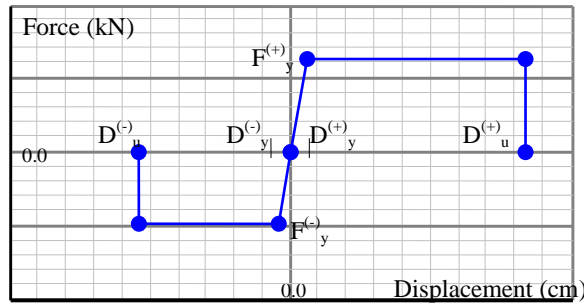


Figure 6. Typical trilinear model adopted for steel bracings

It should be noted at this point that both infill walls and steel braces (whenever included in the models) are placed in the OpenSees script after the application of the gravity loads (according to the seismic combination $G+0.30*Q$) in order to realistically take into account the fact that they are constructed after the load bearing structure made of RC members. If they were included together with the RC structural members, then masonry walls would not simply act as infill panels, but in a diverse manner that would lead to a much different structural behavior. Furthermore, both infills and braces are modeled in this study considering only their in-plane and not their out-of-plane behavior.

4. NUMERICAL RESULTS

4.1 Modal analyses

Initially, a modal analysis of the bare structure was performed and the first four eigenperiods were equal to: $T_1=0.800$, $T_2=0.585$, $T_3=0.532$, $T_4=0.266$. It has to be noted that these values correspond to the assumed reduction of torsional stiffness of columns, as it was previously mentioned, that affected significantly the results of the bare structure (actually the first eigenperiod was mostly affected, about 34% increase for a 50% reduction of torsional stiffness). For the examined four modelling scenarios the effect of torsional stiffness is negligible in the results of modal analysis. After varying the two

basic parameters of the infills, new modal analyses were performed for each examined scenario and the corresponding results are presented in Table 3. It should be noted that values correspond to the initial state of the structure, i.e., before the application of gravity and lateral loads.

Table 3. First eigenperiods of the modelling scenarios

Three first eigenperiods of the 4 modeling scenarios				
	Fully infilled	Open ground floor	Scenario br1	Scenario br2
$\varepsilon_m=0.0010$ $t_{cr}=0.20(\text{kN/m}^2)$	0.447/0.400/0.262	0.547/0.496/0.386	0.374/0.340/0.216	0.285/0.275/0.159
$\varepsilon_m=0.0012$ $t_{cr}=0.20(\text{kN/m}^2)$	0.475/0.430/0.282	0.554/0.448/0.427	0.394/0.376/0.229	0.295/0.283/0.160
$\varepsilon_m=0.0014$ $t_{cr}=0.20(\text{kN/m}^2)$	0.499/0.459/0.300	0.648/0.457/0.434	0.410/0.392/0.241	0.290/0.285/0.162
$\varepsilon_m=0.0010$ $t_{cr}=0.24(\text{kN/m}^2)$	0.419/0.381/0.243	0.598/0.477/0.372	0.356/0.326/0.205	0.277/0.276/0.156
$\varepsilon_m=0.0010$ $t_{cr}=0.28(\text{kN/m}^2)$	0.395/0.365/0.228	0.606/0.461/0.361	0.341/0.327/0.195	0.274/0.273/0.155
$\varepsilon_m=0.0014$ $t_{cr}=0.28(\text{kN/m}^2)$	0.447/0.400/0.262	0.547/0.496/0.386	0.374/0.340/0.216	0.285/0.275/0.159

By inspecting Table 3 it can be easily observed that the differences between the values obtained after the variation of the two parameters of the infills for each modelling scenario are not trivial. In the case of the open ground floor, the variation of ε_m causes higher differences compared to the other modelling cases. Generally, as it was expected, the increase of the deformation parameter ε_m increases the value of eigenperiods (as a result of the stiffness reduction of struts), while the opposite happens when the strength parameter t_{cr} increases. The only exception is the case of the model “Open ground floor”, in which the 1st storey without infills plays a dominant role, hence, the overall behavior is not affected in a direct manner by the variation of the parameters of the infills. It is worth noticing that the values of the first set of the parameters are identical with those of the last set and this is due to the fact that the percentage of the increase of the two parameters is the same, thus, the ratio of Equation (4) remains the same.

4.2 Pushover analyses

Several pushover analyses were performed after applying lateral forces in both directions of the building, for various combinations of infill modeling parameters and examined scenarios (totally 48 analyses) and the results are presented in Tables 4 to 7. The lateral forces were imposed along the height of the building at the center of mass (CM) of each storey, following a pattern proportional to each floor mass according to EC8 – Part 1 provisions, due to the regularity in plan and in elevation of this building as well as the diaphragmatic action of slabs (but without considering any eccentricity).

In each analysis the structure is pushed until the displacement of the top CM (i.e., of the CM of the building’s roof) reaches a high value (different for each modeling scenario) in order to surpass the highest point of the capacity curve and to enable obtaining the maximum value of the base shear when it is clearly reached and then to obtain the corresponding displacement of upper CM and the corresponding drifts of stories. Note that it was not intended to reach numerically the near collapse state, since the numerical models were not adequately formed for this purpose. For instance, the out-of-plane behavior of infills should also be modeled, while a more realistic post-yield behavior represented from the adopted constitutive law for the braces (as well as for RC beams) should be considered. Moreover, the beam-column joints should be simulated in a more elaborate manner, especially for the nodes where the braces are connected.

By inspecting Tables 4 and 5 it is evident that in the case of open ground floor the capacity of the structure is very low in terms of maximum base shear and the corresponding top displacement. Additionally, it can also be observed that in the same case the differences due to the variation of the mechanical parameters of the infills were negligible (in both directions). Such behaviour was expected

as the open ground floor is dominating the overall behaviour of the structure, hence, the influence of modelling parameters of the infills at the upper two stories is not so crucial as the absence of walls at the ground floor. It can also be noticed that for the models “fully infilled” and “scenario br1” there is an increase of the maximum base shear due to the increase of t_{cr} , while this is not the case for the model “scenario br2” for direction +X. The increase of the deformation parameter ϵ_m reduces the base shear for direction +X for “scenario br2”, while for direction +Y there is not a clear trend.

Table 4. Maximum base shear and corresponding roof displacement (direction +X)

Max base Shear (kN) / corresponding Roof Displacement (m) (direction +X)				
	Fully infilled	Open ground floor	Scenario br1	Scenario br2
$\epsilon_m=0.0010$ $t_{cr}=0.20(\text{kN/m}^2)$	660.29/0.075	107.95/0.009	741.20/0.061	1718.66/0.263
$\epsilon_m=0.0012$ $t_{cr}=0.20(\text{kN/m}^2)$	655.23/0.089	108.03/0.010	735.97/0.071	1716.10/0.310
$\epsilon_m=0.0014$ $t_{cr}=0.20(\text{kN/m}^2)$	648.64/0.105	107.57/0.011	734.16/0.083	1416.61/0.076
$\epsilon_m=0.0010$ $t_{cr}=0.24(\text{kN/m}^2)$	768.94/0.080	107.97/0.009	874.83/0.067	1572.23/0.072
$\epsilon_m=0.0010$ $t_{cr}=0.28(\text{kN/m}^2)$	876.98/0.086	107.75/0.007	998.68/0.084	1958.67/0.289
$\epsilon_m=0.0014$ $t_{cr}=0.28(\text{kN/m}^2)$	867.83/0.114	107.77/0.009	994.93/0.114	1965.91/0.319

Table 5. Maximum base shear and corresponding roof displacement (direction +Y)

Max base Shear (kN) / corresponding Roof Displacement (m) (direction +Y)				
	Fully infilled	Open ground floor	Scenario br1	Scenario br2
$\epsilon_m=0.0010$ $t_{cr}=0.20(\text{kN/m}^2)$	824.73/0.160	163.62/0.021	891.40/0.163	2340.54/0.341
$\epsilon_m=0.0012$ $t_{cr}=0.20(\text{kN/m}^2)$	825.32/0.181	162.07/0.022	911.86/0.184	2342.07/0.337
$\epsilon_m=0.0014$ $t_{cr}=0.20(\text{kN/m}^2)$	826.72/0.205	162.37/0.026	929.40/0.178	2346.84/0.347
$\epsilon_m=0.0010$ $t_{cr}=0.24(\text{kN/m}^2)$	900.56/0.181	164.26/0.020	966.21/0.178	2409.28/0.303
$\epsilon_m=0.0010$ $t_{cr}=0.28(\text{kN/m}^2)$	974.66/0.233	164.04/0.021	1062.96/0.290	2506.36/0.421
$\epsilon_m=0.0014$ $t_{cr}=0.28(\text{kN/m}^2)$	1007.03/0.296	163.50/0.020	1062.29/0.236	2478.45/0.427

The roof displacement that corresponds to the max base shear generally follows the increase of both parameters ϵ_m and t_{cr} , as it also increases. Nevertheless, for the model “scenario br2” rather non-characteristic results occur for two specific sets of parameters ($\epsilon_m=0.0014$ & $t_{cr}=0.20\text{kN/m}^2$ and $\epsilon_m=0.0010$ & $t_{cr}=0.24\text{kN/m}^2$). Additionally, the storey drifts for all stories were calculated for each case and they are presented in Tables 6 and 7, from which similar observations can be drawn. It is also evident by observing Tables 6 and 7 that in the case of scenarios “br1” and “br2” the 2nd and/or 3rd storey drifts are more crucial for the overall behavior of the structure than those of the 1st floor, while

for the model “Fully infilled” this is true only for direction +Y. With respect to “Open ground floor” model, the 1st storey drift always plays a dominant role compared to the upper stories, as it was also explained for the results shown in Tables 4 and 5.

Table 6. Storey drifts (1st/2nd/3rd floor) of the modelling scenarios corresponding to the maximum base shear (direction +X)

1 st / 2 nd / 3 rd Storey Drift corresponding to max Base Shear (direction +X)				
	Fully infilled	Open ground floor	Scenario br1	Scenario br2
$\varepsilon_m=0.0010$ $t_{cr}=0.20(\text{kN/m}^2)$	0.015/0.009/0.002	0.006/0.0001/-0.003	0.002/0.015/0.004	0.018/0.035/0.036
$\varepsilon_m=0.0012$ $t_{cr}=0.20(\text{kN/m}^2)$	0.018/0.011/0.003	0.006/0.0001/-0.003	0.002/0.018/0.004	0.021/0.041/0.043
$\varepsilon_m=0.0014$ $t_{cr}=0.20(\text{kN/m}^2)$	0.021/0.013/0.003	0.007/0.0001/-0.003	0.002/0.021/0.005	0.006/0.010/0.010
$\varepsilon_m=0.0010$ $t_{cr}=0.24(\text{kN/m}^2)$	0.016/0.009/0.003	0.007/0.0001/-0.003	0.002/0.015/0.005	0.006/0.009/0.010
$\varepsilon_m=0.0010$ $t_{cr}=0.28(\text{kN/m}^2)$	0.016/0.010/0.005	0.006/0.0001/-0.003	0.003/0.018/0.008	0.020/0.038/0.040
$\varepsilon_m=0.0014$ $t_{cr}=0.28(\text{kN/m}^2)$	0.021/0.013/0.006	0.006/0.0001/-0.003	0.003/0.024/0.012	0.022/0.042/0.044

Table 7. Storey drifts (1st/2nd/3rd floor) of the modelling scenarios corresponding to the maximum base shear (direction +Y)

1 st / 2 nd / 3 rd Storey Drift corresponding to max Base Shear (direction +Y)				
	Fully infilled	Open ground floor	Scenario br1	Scenario br2
$\varepsilon_m=0.0010$ $t_{cr}=0.20(\text{kN/m}^2)$	0.019/0.021/0.015	0.008/0.001/-0.001	0.003/0.026/0.026	0.028/0.044/0.044
$\varepsilon_m=0.0012$ $t_{cr}=0.20(\text{kN/m}^2)$	0.022/0.024/0.016	0.008/0.001/-0.001	0.003/0.032/0.026	0.028/0.043/0.044
$\varepsilon_m=0.0014$ $t_{cr}=0.20(\text{kN/m}^2)$	0.026/0.027/0.017	0.009/0.001/-0.001	0.003/0.034/0.023	0.028/0.044/0.045
$\varepsilon_m=0.0010$ $t_{cr}=0.24(\text{kN/m}^2)$	0.015/0.024/0.023	0.008/0.001/-0.001	0.003/0.022/0.034	0.027/0.040/0.036
$\varepsilon_m=0.0010$ $t_{cr}=0.28(\text{kN/m}^2)$	0.015/0.028/0.036	0.008/0.001/-0.001	0.004/0.046/0.047	0.040/0.053/0.051
$\varepsilon_m=0.0014$ $t_{cr}=0.28(\text{kN/m}^2)$	0.022/0.040/0.038	0.007/0.001/-0.001	0.004/0.039/0.037	0.037/0.054/0.054

5. CONCLUSIONS

In the present work the combined effects of infill walls and steel braces in seismic assessment of RC buildings has been examined, via numerical simulations (utilizing OpenSees) of a prototype RC structure (SPEAR building). The investigation of the overall behaviour of the structure (since the local behaviour of the members was not examined in this study) for the created modelling scenarios has shown that the variation of the strength and deformation parameters of infill walls: i) causes normal

and justified changes for the modelling scenario “Fully infilled”, ii) has insignificant influence for the modelling scenario “Open ground floor”, iii) has in general normal effects for the modelling scenario “br1” (yet, not to the same extent for the two directions), and iv) causes some irregular (and in some cases unexpected) results for the modelling scenario “br2”. A general conclusion that can be drawn is that the results are sensitive to the variation of the mechanical parameters of the infills when infill panels are modelled in conjunction with steel braces and a robust numerical simulation must take place in such cases to obtain a realistic representation of the structural response.

The present investigation demonstrates the complexity and difficulties to predict a priori the efficiency of any strengthening intervention, such as steel bracing retrofitting strategy, in conjunction with the influence of infills. It is also suggested that dynamic non-linear analysis should be performed in order to investigate the hysteretic behaviour of the structure under seismic loading conditions. Furthermore, a more extensive investigation should be made including the variation of additional parameters of infills and not only those that are used to represent strength and deformation values, such as the effective width of the struts, the slenderness of infill panels, etc.

REFERENCES

- Antonopoulos TA and Anagnostopoulos SA (2013) “Improving the seismic performance of existing old pilotis type buildings by strengthening only the ground story”, *Proceedings of COMPDYN 2013, 4th Conference on Computational Methods in Structural Dynamics & Earthquake Engineering*, Kos, Greece, 12-14 June
- Dolsek M and Fajfar P (2005) Post test analyses of the SPEAR test building, Technical Report, University of Ljubljana, Slovenia
- EAK (2003). Greek Seismic Design Code 2000, Greek Organization for Seismic Planning and Protection (OASP). Greek Ministry for Environmental Planning and Public Works, Athens Greece (in Greek)
- EN 1993-1-1 (2005) Eurocode 3: Design of steel structures. Part 1 - 1: General rules and rules for buildings, European Standard EN 1993-1-1:2005, European Committee for Standardization (CEN), Brussels, Belgium
- EN 1998-1 (2004) Eurocode 8: Design of structures for earthquake resistance- Part 1: General rules, seismic actions and rules for buildings, European Standard EN 1998-1:2004, European Committee for Standardization (CEN), Brussels, Belgium
- EN 1998-3 (2005) Eurocode 8: Design of structures for earthquake resistance Part 3: Assessment and retrofitting of buildings, European Standard EN 1998-3:2005, European Committee for Standardization (CEN), Brussels, Belgium
- Fragiadakis M, Lanese I, Pavese A and Papadrakakis M (2009) “Experimental and numerical investigation of a reinforced concrete building designed for gravity loads only”, *Proceedings of COMPDYN 2009, 2nd Conference on Computational Methods in Structural Dynamics & Earthquake Engineering*, Rhodes, Greece, 22-24 June
- Hashemi A and Mosalam K.M (2006) “Shake-table experiment on reinforced concrete structure containing masonry infill wall”, *Earthquake Engineering & Structural Dynamics*, 35: 1827-1852
- KAN.EPE (2013) Code of structural interventions on reinforced concrete buildings, English version after harmonization with Eurocode 8 Part 3, Earthquake Planning and Protection Organization (E.P.P.O), Athens, Greece, available at <http://ecpfe.oasp.gr/>
- Kappos AJ and Panagopoulos G (2009) RCCOLA.NET: Program for the inelastic analysis of RC cross-sections: User’s Manual, Civil Engineering Department, Aristotle University of Thessaloniki, Greece (in Greek)
- McKenna F, Fenves G and Scott M (2000) OpenSees: Open system for earthquake engineering simulation, Pacific Earthquake Engineering Research Center (PEER), University of California Berkeley, CA
- Mondal G and Tesfamarian S (2014) “Effects of vertical irregularity and thickness of unreinforced masonry infill on the robustness of RC framed buildings”, *Earthquake Engineering & Structural Dynamics*, 43: 205-223
- RAF-TOL (2013) RAF-TOL: Program for the analysis of buildings: User’s Manual Version 4.1, TOL Software Co, Heraklion, Greece (in Greek)
- SPEAR (2005) “Seismic performance assessment and rehabilitation of existing buildings”, *Proceedings, of International Workshop*, Fardis M and Negro P (eds), 4-5 April 2005, Ispra, Italy
- Uva G, Porco F and Fiore A (2011) “Appraisal of masonry infill walls effect in the seismic response of RC framed buildings: A case study”, *Engineering Structures*, 34: 514-526
- Zarnic R and Gostic S (1997), “Masonry infilled frames as an effective structural sub-assembly”, In Seismic design methodologies for the next generation of codes, Fajfar P and Krawinkler H (eds), Balkema, Rotterdam, pp. 335-346